BIOCHEMISTRY
including biophysical chemistry & molecular biology

ARTICLE

pubs.acs.org/biochemistry

Adaptive MscS Gating in the Osmotic Permeability Response in *E. coli*: The Question of Time

Miriam Boer, Andriy Anishkin, and Sergei Sukharev*

Department of Biology, University of Maryland, College Park, Maryland 20742, United States

Supporting Information

ABSTRACT: Microorganisms adapt to osmotic downshifts by releasing small osmolytes through mechanosensitive (MS) channels. We want to understand how the small mechanosensitive channel's (MscS) activation and inactivation, both driven by membrane tension, optimize survival in varying hypoosmotic shock situations. By measuring light scattering with a stopped-flow device, we estimate bacterial swelling time as 30−50 ms. A partial solute equilibration follows within 150−200 ms, during which optical responses from cells with WT MscS deviate from those lacking MS channels. MscS opening rates estimated in patch clamp show the channels readily respond to tensions below the lytic limit with a time course faster than 20 ms and close promptly upon tension release. To address the role of the tension-insensitive inactivated state *in vivo*, we applied short, long, and two-step osmotic shock protocols to WT, noninactivating G113A, and fast-inactivating D62N mutants. WT and G113A showed a comparable survival in short 1 min 800 mOsm downshock experiments, but G113A was at a disadvantage under a long 60 min shock. Preshocking cells carrying WT MscS for 15 s to 15 min with a 200 mOsm downshift did not sensitize them to the final 500 mOsm drop in osmolarity of the second step. However, these two-step shocks induced death in D62N more than just a one-step 700 mOsm downshift. We conclude MscS is able to activate and exude osmolytes faster than lytic pressure builds inside the cell under abrupt shock. During prolonged shocks, gradual inactivation prevents continuous channel activity and assists recovery. Slow kinetics of inactivation in WT MscS ensures that mild shocks do not inactivate the entire population, leaving some protection should conditions worsen.

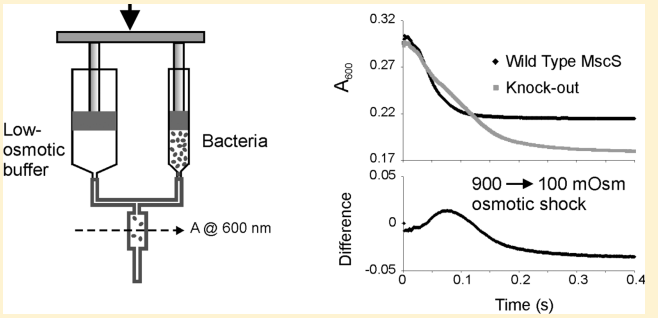

Free-living and enteric bacteria possess adaptive mechanisms to survive drastic environmental osmotic changes. Under high osmolarity, bacteria initially accumulate K^+, followed by replacement of ions with compatible organic osmolytes (for example, proline, betaine, and trehalose).[1,2] When the external osmolarity suddenly drops and water rushes into the cells, bacteria regulate the increased turgor and volume by releasing excessive osmolytes through mechanosensitive channels. Four known channels regulate the system: the mechanosensitive channel of miniconductance (MscM),[3] the potassium-dependent mechanosensitive channel (MscK),[4] the mechanosensitive channel of small conductance (MscS), and the large mechanosensitive channel (MscL).[5−7] Out of these four, MscS and MscL appear to regulate the bulk of turgor-driven solute release. If either MscS or MscL alone is present in the cell membrane, cells easily survive abrupt osmotic downshock.[8] Both channels are gated by tension in the lipid bilayer, although they are structurally unrelated.[9−11] MscL, with 3 nS conductance, opens at near-lytic tensions (9−15 mN/m). Although MscL shows some adaptation in excised patches,[12] it does not inactivate and exhibits steady activity under constant tension above the threshold. MscS conducts at 1 nS and opens under moderate sub-lytic tensions (5−8 mN/m).[9,12,13] In excised patches, MscS does not show sustained activity at constant tension; it shows transient adaptive responses which result in complete inactivation. It appears to mediate most turgor-limiting osmolyte exchange under non-lytic conditions. In many "wild-type" *Escherichia coli* strains, MscL is constitutively produced at the level of 5−10 copies per cell, but MscS can be 2−5 times more abundant. Both genes, *yggB* (*mscS*) and *mscL*, are under control of RpoS (σs), a stress-mediating transcription factor.[14]

Both MscS and MscL are large and essentially nonselective channels, so every opening event dissipates vital gradients and comes at a metabolic cost. MscS' transient responses resulting in the inactivated state likely prevent leaks under sub-lytic tension. This adaptive behavior is evident when pressure is applied gradually, and only a fraction of the MscS population opens in contrast to full-scale responses from abrupt transmembrane pressure steps.[15,16] Both activation and inactivation are triggered by membrane tension with approximately the same threshold but different kinetics,[15] usually allowing the channel to open first and then gradually inactivate under persisting moderate tension.

Received: December 6, 2010
Revised: March 29, 2011
Published: April 01, 2011

While the existing crystal structures of WT[17] and A106 V[18] MscS provide staring points for the modeling of the MscS's transitions assisted by EPR[19,20] or new computational techniques,[21,22] detailed functional analysis of opening and inactivation[16,23] remains an indispensable part of our understanding of the MscS gating cycle and its structural underpinning. The biological question is whether and how inactivation gives an adaptive edge to bacteria subject to short, prolonged, or gradual osmotic challenges.

Previously, most osmotic shock viability tests were performed on cultures pre-equilibrated in high-osmotic media by rapidly mixing them with low-osmolarity media and plating them on agar plates within 1−5 min.[8,24] This simple one-step shock scenario with quick plating is similar to a single saturating pressure pulse on patch clamp, not necessarily revealing inactivation. But the osmotic conditions in natural habitats vary. For instance, when it rains, soil bacteria at the surface would experience very different dilution kinetics from bacteria below the surface. Enteric bacteria cycling between intestines and soil live in especially complex osmotic regime. No data currently addresses the differences between abrupt and gradual shocks. Bacteria are small and are expected to swell quickly, but how the time course of tension development and decline compares to the activation, closure, and inactivation kinetics of MscS in different shock regimes is unknown. All these parameters may influence survival.

To address the roles of normal MscS activation and inactivation in osmotic survival, we performed stopped-flow experiments to determine characteristic swelling and lysis times under "instant" mixing and compared them to patch-clamp data under machine-driven tension application. We then designed parallel patch-clamp and osmotic dilution plating experiments with wild-type (WT) bacteria, along with a noninactivating mutant, G113A,[16] and a fast inactivating mutant, D62N,[25] and tested their viability in four different regimes of osmotic shock.

We chose these mutants based on previous studies[16,25,26] suggesting at least two loci involved in inactivation. The first locus is the flexible hinge at G113 on the third transmembrane helix (TM3), shown to be involved specifically in inactivation.[16,26] MscS' closed-to-open transition was inferred as straightening and tilting of the pore-lining TM3 helices,[16,22] whereas the return to a nonconductive state was associated with buckling of TM3 at one of the flexible points, either G113 during inactivation or G121 during closing.[16] Higher helical propensity in the hinge region imposed by the G113A substitution nearly abolished inactivation, thus generating a model noninactivating mutant. The second site was D62 at the tip of the TM1−TM2 loop, which was proposed to form a salt bridge with the R128/R131 cluster on the "cage".[25,27] The feasibility of the D62−R131 salt bridge formation is illustrated by a model presented in Figure S1. Disruption of these salt bridges by D62N/R mutations leads to fast adaptation of the channel[25] and, as will be shown below, inactivation as well. The conformational coupling between the transmembrane and cytoplasmic "cage" domains supporting the presence of the salt bridge was also disrupted by the D62N mutation.[28] D62N MscS was thus chosen as a model fast inactivator. The aim of the following experiments involving these mutants is to compare the inactivation times and demonstrate the importance of inactivation in the functional cycle of MscS *in vivo*.

MATERIALS AND METHODS

Strains and Mutants. WT MscS and the mutants were expressed in MJF465 triple knockout (KO) (*mscS*$^-$, *mscL*$^-$, *mscK*$^-$) cells[8] from the pB10b vector as described previously.[9,29] D62N originally studied in ref 25 was kindly provided by Dr. K. Yoshimura. Control MJF465 cells (KO) carried empty pB10b vector. For *in vivo* experiments, the overnight culture was diluted 1:1000 in high-osmotic medium (HiLB: 900 mOsm LB; we increased osmolarity with addition of 0.5 M NaCl) and grown for 2 h to optical density OD_{600} of 0.4. The cells were induced at 1.5 h with IPTG for 30 min, collected, and then diluted into low-osmotic medium in different settings.

Stopped-Flow Measurements. Cells pregrown and induced in HiLB were washed twice in Tris-buffered 900 mOsm NaCl solution (pH 7.2) and resuspended in the same buffer at OD 0.6. An Applied Photophysics SX18MV stopped flow machine was used to detect changes in light scattering through recording the absorbance at a wavelength of 600 nm (detection at 180°, 190 V setting on PMT). The cell suspension was instantly mixed with NaCl solutions of varying osmolarity at the volume ratio of 1:10, delivered from 0.2 and 2 mL syringes. The light absorbance was recorded for 1 min after rapid mixing, and traces from 10 consecutive trials were averaged.

Osmotic Survival Assays. For single shock experiments, cells grown in HiLB were hypoosmotically downshocked in either LB/2 (200 mosm) or LB/4 (100 mosm). We made a 1:100 dilution from HiLB directly to LB/2 or LB/4 and let the bacteria adjust. The cells were further diluted (1:1000) in the respective low-osmotic medium, and 150 μL was plated first at 1 min and again at 60 min. Controls were diluted the same way in HiLB and plated. All plates were incubated overnight and colonies counted the following morning. All experiments represent data of at least five independent experiments with plating in duplicates.

For double shock experiments, cells grown in HiLB were hypoosmotically downshocked first in 700 mosm LB for 15 s, 1 min, and 15 min, followed by a more severe downshock in either LB/2 or LB/4 for 15 min. Then, after reaching the identical dilution as the single shock experiments, 150 μL samples were plated on LB plates. Two controls were used in these experiments. The primary control was diluted to the same concentration in HiLB and plated. The secondary control was a 15 min long single shock to either LB/2 or LB/4, identically diluted. As above, they were incubated overnight and the colonies counted the following morning. All percent survival calculations were done with the unshocked control taken as 100% survival.

Electrophysiology and Analysis. Giant spheroplasts were generated using the modified cephalexin method[15,25] with a 30 min induction by IPTG (0.8 mM). Patch-clamp recordings were taken using the same device and pipettes as outlined in Akitake et al.[15] Programmed pressure protocols were delivered from an HSPC-1 pressure-clamp apparatus (ALA Instruments). All recordings were done at +30 mV in the pipet in symmetric 200 mM KCl, 90 mM $MgCl_2$ and 10 mM $CaCl_2$, 5 mM HEPES buffer (pH 7.2). After seal formation and excision, inside-out patches were subjected to 1 s linear pressure ramps, and the midpoint for activation ($p_{0.5}$) was determined. We assumed that in the range of activating tensions patch curvature is constant and thus tension in the membrane (γ) depends linearly on patch radius (r) and pressure gradient (ΔP) according to Laplace's law ($\gamma = \Delta P r/2$). For each patch individually we converted pressure into tension using the MscS tension midpoint $\gamma_{0.5}$ = 7.8 mN/m previously determined in whole-spheroplast experiments.[12]

The thermodynamic analysis of traces was done according to two-state Boltzmann equation $P_0 = 1/(1 + \exp((\Delta E - \gamma \Delta A)/kT)$, where ΔE and ΔA are the changes in free energy and

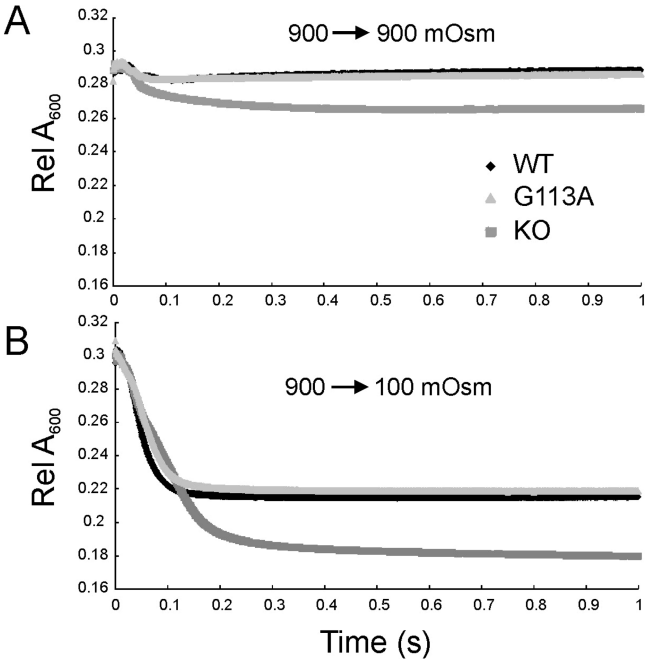

Figure 1. Stopped-flow experiment with MJF 465 cells expressing WT MscS, G113A MscS, or empty pB10b vector (KO). One second traces show the dynamics of light scattering for the three cultures under no shock (900 → 100 mOsm, A) and under extreme downshock (900 → 100 mOsm, B).

in-plane area of the protein associated with the opening transition, k is the Boltzmann constant, and T is absolute temperature. The partial area changes between the closed (C) and open (O) conformations and the transition barrier (B) were estimated from the tension dependencies for the opening and closing rates: $\Delta A_{C\rightarrow B} = kT\ d\ \ln(k_{on})/d\gamma$ and $\Delta A_{O\rightarrow B} = kT\ d\ \ln(k_{off})/d\gamma$.[30]

Molecular Modeling. The D62-R131 salt bridge in MscS was first proposed in ref 27 for conformation derived from the crystal structure. The feasibility of this salt bridge for a compact resting state[16,21] was suggested by the molecular model presented in Figure S1 along with the technical details of computation.

RESULTS

To explore the kinetics of bacterial swelling and tension onset in fast dilution experiments, we measured light scattering dynamics from the bacterial suspension with the stopped flow technique. On the basis of this data, we chose settings for patch-clamp experiments to comparably stimulate MscS over similar characteristic times in isolated membrane patches.

In the osmotic stopped-flow experiment, a small volume of dense *E. coli* suspension grown in 900 mOsm LB and equilibrated in a NaCl Tris-buffered medium of the same osmolarity was rapidly mixed with a 10× volume of lower-osmolarity buffer to obtain a final optical density between 0.07 and 0.05. The 10× averaged traces of the strongest shock (900 → 100 mOsm) are shown in Figure 1 for the three strains (WT, G113A, and KO) in comparison with no shock responses. From absorbance kinetics one can see that unshocked control (900 → 900 mOsm, Figure 1A) shows a small ~20 ms spike of optical density in WT and G113A strains, perhaps a mixing artifact or a result of cell orientation in the flow, followed by a stable absorbance in the end state. KO cells reproducibly featured a slow decrease of optical density likely caused by shear stress in the flow or by dilution from a self-conditioned dense suspension. When severely shocked, (900 → 100 mOsm, Figure 1B), the traces for WT and G113A show a drop of optical density within ~150 ms with a quick stabilization at a new level. The KO strain shows a deeper and slightly delayed decrease of OD with no visible stabilization of the end state within 1 s. We presume that rapidly entering a hypoosmotic solution induces cell swelling followed by osmolyte release. Swelling increases cell size, which can increase scattering, but at the same time swelling dilutes the cytoplasm, thus decreasing refractive index and scattering. In cells containing WT MscS, we expect MscS to respond to swelling with a rapid osmolyte efflux, whereas in the unprotected KO cells, which lack MscS and two other MS channels, severe osmotic downshock was expected to cause osmolyte efflux through nonspecific membrane cracks and lethal damage.[8]

As seen from Figure 1B, the traces for WT and the G113A noninactivating mutant essentially coincide, quickly stabilizing at a new level. The WT's ability to inactivate does not produce any substantial difference in optical responses compared to the noninactivating G113A, suggesting the massive release of osmolytes occurring in this time scale does not involve inactivation. The stabilization of absorbance after the initial drop likely represents channel closure upon pressure release. The fast-inactivating D62N mutant exhibited a partial loss-of-function phenotype compromising viability at these shocks;[25] for this reason it was not included in these trials. In the following experiments we compared the responses of WT MscS-expressing bacteria with the KO strain devoid of three major MS channels.

Four trials with a progressively increasing amplitude of shock (Figure 2) show decreasing optical density due to decreased scattering. Under no shock conditions, the KO cells reproducibly featured a slow decrease of optical density, and as a result, the difference trace (KO minus WT, bottom of each panel) shows a gradual decrease. The 900 → 500 mOsm dilution shows a biphasic response in both WT and KO cells, with a fast scattering drop that similarly completes within ~50 ms and a slower phase that is slightly delayed in KO; the difference trace bulges up with a shallow maximum near 150 ms. Shocking from 900 to 200 mOsm produces a considerably deeper but slower drop of scattering for KO with a more pronounced difference peak near 100 ms. The final most extreme 900 → 100 mOsm shock produces a similar response with a delayed "shoulder" in KO cells, which produces a sharper difference peak.

Cell survival determined under shocks of the same magnitude (Figure 2C) shows KO viability drops precipitously under a 900 to 200 mOsm downshock, whereas cells expressing WT MscS survive and experience significant viability loss only when downshocked from 900 to 100 mOsm. The first notch in the light scattering data in both cultures' responses may reflect mixing/shearing events, while the short plateau and the beginning of scattering drop represent the period of cell swelling (dilution of internal content) when pressure/tension are building up. Figure 2B represents the beginning of the same response plotted as the inverse absorbance (A^{-1}) known to be linearly related to the cell volume ($dV/dt = k(dA^{-1})/dt$, where k is a constant[31]). The empirical relationships between absorbance and volume had been worked out for lipid vesicles[31] and mitochondria[32] which behave largely as ideal osmometers. Since *E. coli* cells are surrounded by elastic cell wall,[33] we do not expect them to behave as osmometers, and thus direct calibration of the scattering response against equilibrium cell volume is difficult. In the course of the first

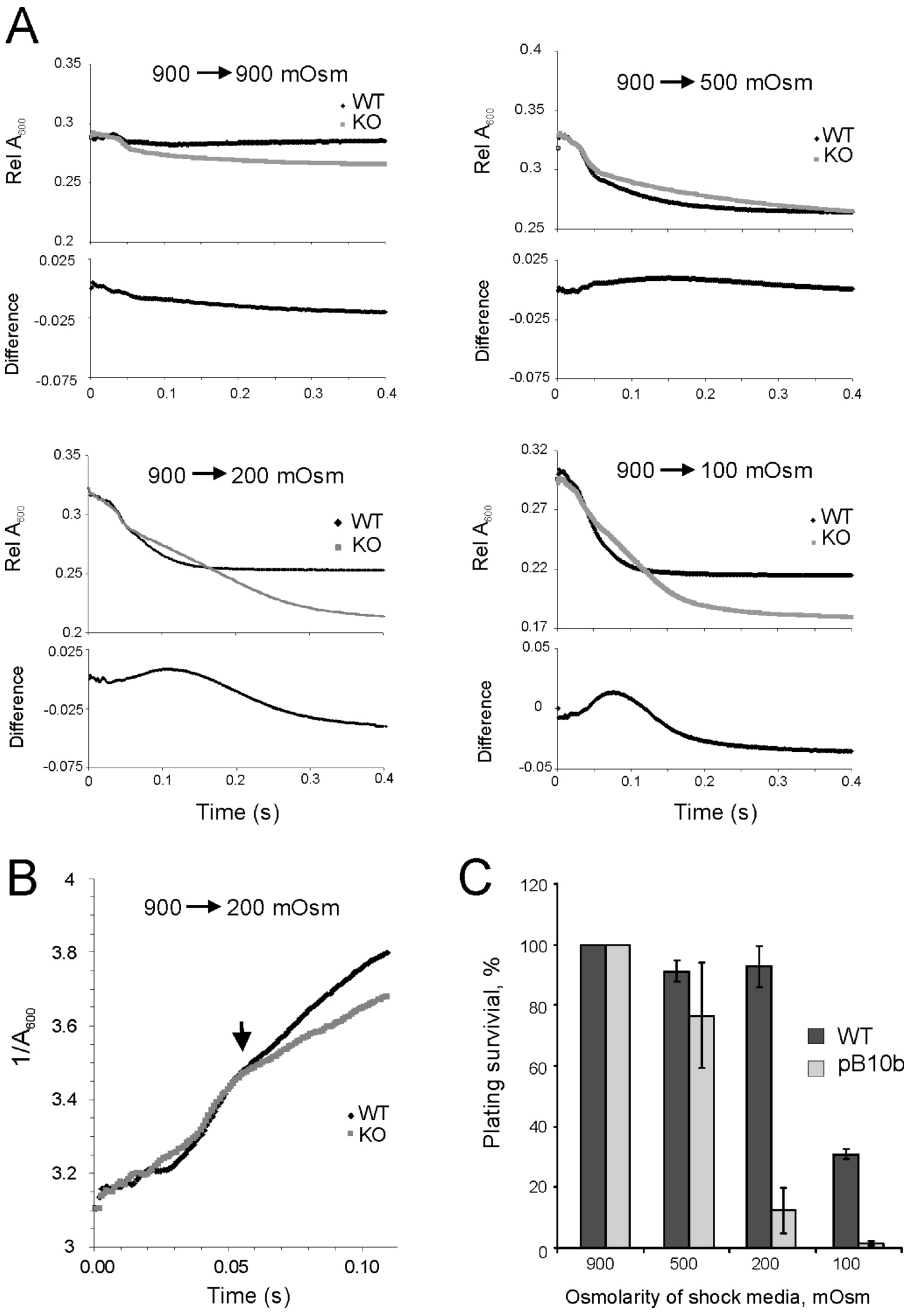

Figure 2. Bacterial swelling response in a stopped flow apparatus correlates with osmotic survival. The smaller syringe contained a dense suspension of *E. coli* cells preadapted at 900 mOsm, and the larger syringe contained buffers of varying osmolarity. (A) Absorbance (A_{600}) traces from MscS WT and from empty vector control (KO) injected at the same density. Data show a time-dependent decrease of scattering (top panels). Lower traces in each set represent the difference between WT and KO responses. Under strong shocks (900 → 200 and 900 → 100 mOsm), KO cells loose viability and the difference peak reflects osmotic damage following swelling. (B) Inverse absorbance (A^{-1}) in the 900 → 200 mOsm as a function of time; the arrow shows the 50 ms time point at which the traces deviate marking the onset of permeability. (C) Osmotic survival of *E. coli* cells under similar shock conditions as determined with plate counts. Plating was done 10 min after dilution. Error bars represent standard deviation (n = 5).

50 ms, A^{-1} in both WT and KO cultures increases concomitantly by ~10% reflecting swelling (Figure 2B), but after that point (arrow) the traces deviate. WT's further fast scattering drop likely reflects osmolyte efflux through activated channels, which stops when pressure is partially relived and channels close. The deeper, slower, and continuing scattering drop in KO likely indicates leaks through membrane tears, which do not reseal in the time course of 0.4 s (no plateau). The deeper drop of scattering in KO likely indicates more swelling and/or continuing loss of intracellular constituents. The difference peak on each panel is roughly proportional to the difference in the fraction of dead cells (Figure 2C) and may reflect the time course of irreversible osmotic damage. From the traces we conclude that the time of swelling/pressure buildup can be estimated as 30−50 ms, whereas the time of nonlethal equilibration (in WT) shortens with the shock amplitude and reaches completion between 100 and 300 ms.

Thus, MscS should respond rapidly to the 30 ms pressure buildup, and the slope of channel activation rate as a function of

dx.doi.org/10.1021/bi1019435 |*Biochemistry* 2011, 50, 4087–4096

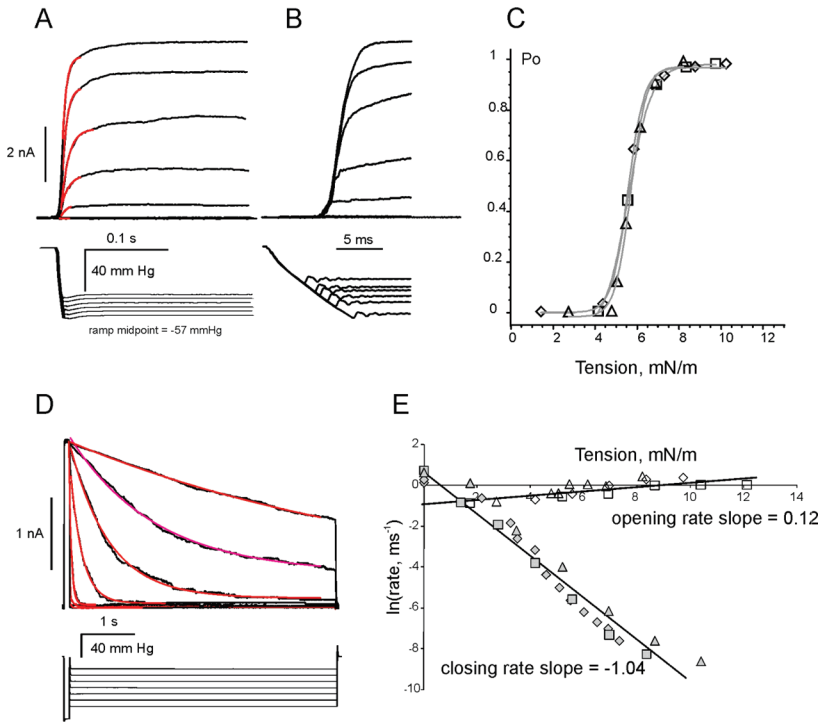

Figure 3. Tension dependencies of MscS opening and closing. (A) Kinetics of MscS opening in response to a series of pressure steps (10 ms raise time). (B) Expanded initial region of the traces in (A) illustrating current onset. (C) The dose−response curve (Po(γ)) obtained from the steady-state current levels in (A) fitted with Boltzmann equation that predicts the energy gap between the states ΔE = 14.5 kT and the in-plane protein expansion ΔA = 10.5 nm^2. (D) Kinetics of MscS closure at different pressures after opening by a short saturating pulse. (E) Tension dependencies of the opening and closing rate constants obtained from monoexponential fits of traces in (A) and (B) shown in red. The opening (open symbols) and closing (filled symbols) rates are shown for three independent patches and fitted together. The slope of the apparent opening rate suggests $\Delta A_{C\rightarrow B}$ = 0.5 nm^2 in-plane expansion between the closed-state well and rate-limiting barrier and the closing rate dependency predicts $\Delta A_{O\rightarrow B}$ = 4.3 nm^2 for the area change from the open well to the barrier. Note that the sum of $\Delta A_{C\rightarrow B}$ and $\Delta A_{O\rightarrow B}$ is less than total ΔA predicted by the Boltzmann fit of the instantaneous dose−response curve (C).

tension would determine the response speed. Another question is how quickly the channel will close if tension drops from a superthreshold level to some intermediate subthreshold level following osmolyte release. We have attempted directly assessing MscS' opening and closing rates under step pressure protocols delivered from a pressure-clamp apparatus. Figure 3A shows a series of patch current responses to 0.2 s long pressure steps of increasing amplitude. The red color indicates the segments of traces fitted with monoexponential functions, approximating opening rates. The expanded current and pressure stimulus traces (Figure 3B) indicate that the machine-limited pressure onset is not instantaneous, but rather is a nearly linear ramp with the slope of ~5 mmHg/ms. The threshold of about 45 mmHg for that particular patch is reached within 8 ms, and the first superthreshold step activates ~15% of channel population within 2 ms. Further pressure buildup increases the fraction of active channels, and the current grows concomitantly with pressure, but each time the current quickly levels off. The exponential fits in Figure 3A show that the apparent initial rate is in the order of ms^{-1}, which increases shallowly with increasing pressure (Figure 3E). The onset of pressure stimulus is obviously not fast enough to resolve the first-order kinetics of MscS as the current closely follows the changing pressure stimulus. The slow onset of pressure may thus underestimate the intrinsic rate of MscS opening, which appears to be faster than indicated in Figure 3E. Yet, the experiment shows that MscS is able to respond quickly to 10−15 ms ramps of pressure and reach 90% of activity within 5 ms, beating cell swelling. The fast response to sub-lytic tension ensures that the "valve" will open and release before the intracellular pressure reaches the lytic limit in the event of abrupt dilution.

Using the steady-state levels obtained at different tensions (Figure 3A), we created a dose−response curves, represented in Figure 3C. Fitting this curve with the two-state Boltzmann equation (see Methods) estimated the energy gap between the open and closed states (ΔE) as 14.5 ± 0.8 kT and the in-plane area change (ΔA) as 10.5 ± 0.5 nm^2 (n = 3), consistent with previous results.[12,15]

Figure 3D shows the closing kinetics recorded with a two-pulse protocol. The first short saturating pulse opens the entire population (~100 channels) in the excised patch, whereas the following longer step of variable amplitude conditions the closing process. Closing of MscS is slower than opening and is well resolved. From the exponential fits of the decaying currents (red lines, panel D), we determined the closing rate dependency on tension (Figure 3E). The slope predicts that the conformation representing the rate-limiting barrier for closing has ~4.3 nm^2 smaller footprint in the plane of the membrane than the open conformation ($\Delta A_{O\rightarrow B}$). Given that the total in-plane expansion (ΔA) of the protein is ~10.5 nm^2, this distance predicts that the rate-limiting barrier is positioned roughly two-thirds of the expansion trajectory toward the open state. Note that the tension dependency of the opening rate was not adequately measured with the available pressure protocol and thus the deduced area

dx.doi.org/10.1021/bi1019435 |*Biochemistry* 2011, 50, 4087–4096

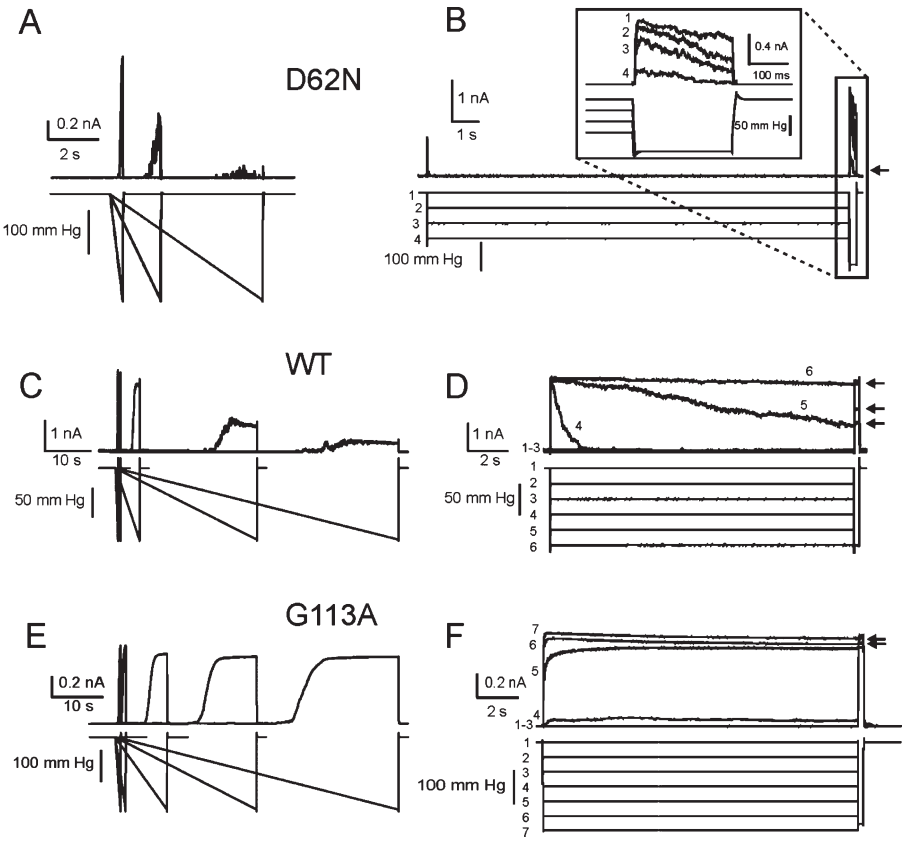

Figure 4. Inactivation of WT MscS and the D62N and G113A mutants as observed by two protocols. The first protocol (panels A, C, E) involved saturating ramps of various durations. The second protocol (B, D, F) was a 15 s preconditioning step followed by a short saturating pulse revealing the noninactivated fraction of the channel population. D62N shows increased inactivation relative to WT in ramp experiments (A) and a silent inactivation bypassing the open state under pulse stimuli (B). G113A shows virtually no inactivation (E, F).

change from the closed well to the rate-limiting barrier ($\Delta A_{C\rightarrow B}$ = 0.5 nm^2) is severely underestimated (Figure 3E and legend). Even in the simplifying assumption of single-barrier transition in MscS,[34] we do not expect that the sum of $\Delta A_{C\rightarrow B}$ and $\Delta A_{O\rightarrow B}$ should correspond to the total ΔA predicted by the Boltzmann fit of the instantaneous dose−response curve (Figure 3C).

The tension dependency of the closing rate (Figure 3E) permits a rough estimation of the residual tension in the cell membrane after the shock. If we take 200 ms as a characteristic time for the osmotic equilibration process completion, then, after activating at 8−10 mN/m, the tension may drop to the residual level of 3−3.5 mN/m to ensure the closing process with this characteristic time. Tension in the membrane does not have to drop to zero, it should simply be 1−2 mN/m below the threshold of ∼5 mN/m (Figure 3C).

Next we addressed the time course and nature of MscS inactivation, which is normally a slow tension-driven process.[15] The physiological meaning of MscS inactivation has not been addressed, and we hypothesize it might be important for cell survival under mild or gradually imposed shocks. The two-syringe stopped-flow technique, however, does not permit us to observe the light scattering changes that would happen in the event of slow or multistep dilution. By comparing inactivation kinetics in WT and mutants with both fast- and noninactivating phenotypes on patch clamp and *in vivo* shock experiments, we evaluated whether WT's slow adaptive behavior confers a survival advantage.

As mentioned in the Introduction, we took cues from the models shown in Figure S1 to choose the mutants for our studies. Previously, the D62−R131 salt bridges were predicted from functional studies[25,28] but were not present in either the crystal structure[17,35] or in the compact models of the resting state.[20,21] The model derived using EMP confirms the possibility of salt-bridge formation, which likely stabilizes TM2−TM3 interactions providing a mechanical link between the lipid-facing helices and the gate.[23] This conformation is also predicted to stabilize the absence of G113 kinks in the resting state. Disruption of the salt bridges by the D62N substitution possibly destabilizes the TM2−TM3 association and increases the probability of G113 kink formation leading to inactivation. Higher helical propensity in the G113A mutation, on the other hand, precludes inactivation.[16]

Figure 4 shows patch-clamp traces recorded from the fast inactivating mutant D62N, WT, and the noninactivating mutant G113A responding to both saturating ramps of varying duration and a prolonged subsaturating pressure step followed by a saturating pulse. From the saturating ramp data, we see the entire channel population on a patch responds to a short ramp, evident from the high conductance level. As the ramps become progressively longer, the maximal current achieved diminishes in both the fast inactivating D62N as well as WT (panels A and C). For example, WT shows only 15% of maximum conductance with a 60 s ramp, so ∼85% of the WT channel population is inactivated. The other protocol, the 15 s pressure step, shows the inactivated MscS fraction depends not only on speed of onset of pressure stimuli but also on sustained subsaturating pressure (Figure 4B,D,F). While current can decline as a result of

dx.doi.org/10.1021/bi1019435 |*Biochemistry* 2011, 50, 4087–4096

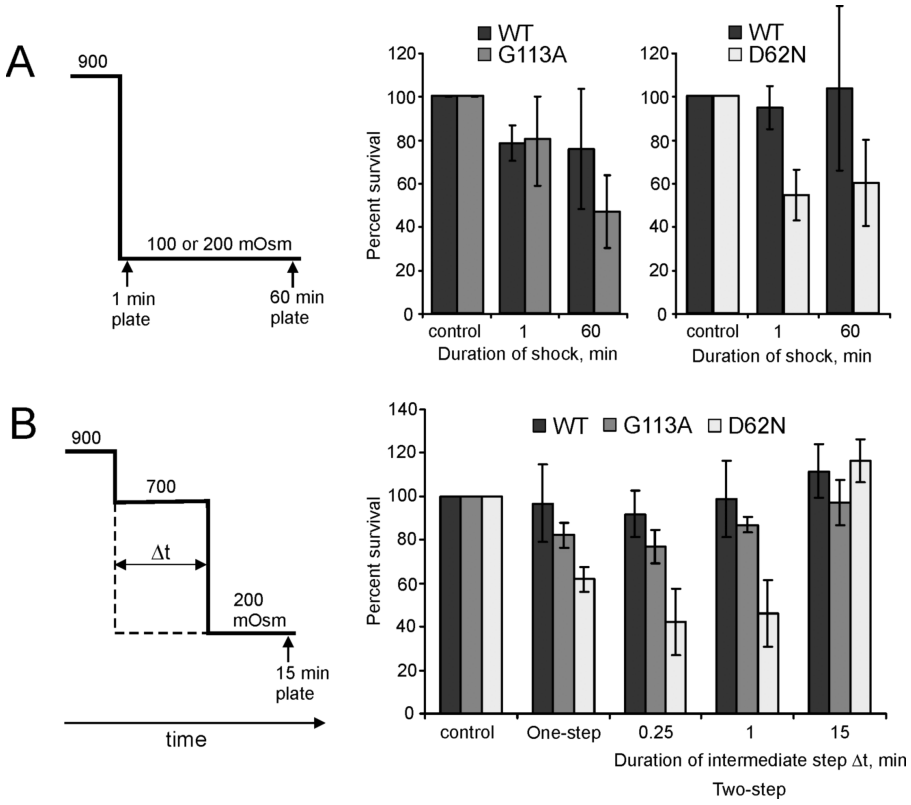

Figure 5. Survival of *E. coli* MJF465 cells expressing WT MscS, noninactivating G113A, or fast-inactivating D62N mutants in different regimes of osmotic shock. (A) Dependence of WT and G113A survival on the duration of exposure to low-osmotic medium (1 or 60 min) after the 900 → 100 mOsm shock. The values for WT (79 ± 24%) versus G113A (47 ± 19%) at 1 min are statistically indistinguishable ($n = 6$), whereas at 60 min the values were different with a t test value of 0.07. The viabilities for G113A at 1 min (82 ± 22%) and 60 min were different with a t test value of 0.02. D62N was shocked into 200 mOsm along with WT controls. The survivals after 1 and 60 min for both strains were the same. (B) The average percent survival of WT, G113A, and D62N when subjected to a 15 min single shock and double shocks of varying duration. D62N has the lowest survival under the two-step shock regime. The error bars represent standard deviations ($n = 6$). The D62N data for the 0.25 and 1 min double shocks are different from one-step shock data with a t test value of 0.09.

reversible adaptation,[12,16] we differentiate between nonconducting responsive (adapted) channels and nonconducting inactivated channels with a short saturating test pulse at the end of the 15 s step. Inactivated channels do not respond. Maximal inactivation was observed at higher pressures still permitting adaptive closure since normally MscS inactivates from the closed state when subjected to tension,[36] and inactivation onset essentially coincides with the activation threshold. Overall, a 15 s constant-pressure stimulation thus is capable of driving about 50% of the WT population to the inactivated state (Figure 4D). Traces obtained with similar protocols for G113A show less than 10% inactivation during 15−60 s stimulation. In the case of the fast-inactivating D62N, 90% of the channels inactivate with a 5 s saturating ramp, which is an order of magnitude faster than WT. D62N also exhibits silent inactivation, which is inactivation under subthreshold tensions bypassing the open state. Only the highest amplitude step (Figure 4B) invokes a brief transient response, but the test pulse in the end reveals that ∼80% of the population is inactivated. On the basis of these observations, we conclude that D62N MscS inactivates much faster when conditioning tension approaches or exceeds the activating threshold.

To reveal the differences in cell survival caused by different inactivation time courses, in the first experiment, we subjected all three strains to intense "short" (1 min) and "long" (60 min) osmotic shocks (Figure 5A) followed by plating on regular LB plates. With a downshift from 900 to 100 mOsm, WT and G113A survived comparably 1 min shock (∼80%), but the longer exposure resulted in a lower survival of G113A. D62N was previously reported to have a higher activation threshold and partial loss-of-function phenotype,[25] and hence its survival in the same shock medium was too low to draw meaningful conclusions about its behavior. For this reason, it was only shocked from 900 to 200 mOsm. The survival of this mutant did not decline with the time of exposure to low osmolarity (Figure 5A, right panel).

The second, two-step protocol was designed to mimic gradual osmolarity downshift (Figure 5B). Bacteria pre-equilibrated at 900 mOsm were first subjected to a 900 → 700 mOsm preshock, and then, after a varied period at intermediate osmolarity (Δt), they were further diluted down to 200 mOsm. The survival of WT and G113A was not substantially compromised by the exposure to the intermediate osmolarity, but the fast inactivator showed a minimum of survival at Δt = 0.25 min (15 s). The data suggest the inactivating mild preshock increases fatalities from the final shock, and it affects D62N significantly more than both WT and G113A.

DISCUSSION

On the basis of the small size and large surface area-to-volume ratio, it was always assumed that osmotic swelling of bacteria should be faster than a second, but characteristic time

measurements can hardly be found in the literature. Previously, stopped flow was used to study solute transport processes in bacteria[37,38] but not fast osmotic swelling. Here we presented light scattering responses of high-osmolarity adapted *E. coli* populations upon rapid (~3 ms) mixing with a hypotonic medium. How a cell suspension scatters light depends on the size, shape, and refractive index of the cells.[39] Consistent with previously reported data for mitochondria[32] and vesicles,[31] the major effect of hypoosmotic shock is decreased scattering. This is largely a result of cytoplasmic dilution due to swelling and subsequent osmolyte efflux. When rod-shaped bacteria delineated by an elastic cell wall swell, we believe there is no dramatic dimensional change. Instead, they may become slightly rounded. When shocked, light scattering time courses for the MscS-expressing and control knockout (KO) cells initially coincide (Figure 2A,B). This suggests that the first 30−50 ms stage where scattering drops by 7−10% reflects cell swelling, which does not involve MscS activation. The subsequent deviation of traces—apparent in the steeper scattering decrease in MscS-expressing cells—likely reflects rapid ion and small osmolyte efflux through activated channels. It signifies that swelling at this time generates superthreshold tension, and the high slope of signal change likely reflects the maximal open probability. The optical response of MscS-expressing cells plateaus in 100−150 ms, which may indicate that either tension is now below the threshold and the channels are closed or the pool of permeable osmolytes is exhausted and the cell size and refractive index do not change anymore. Without detailed calibration of the optical response of cell suspensions[31,32] we were unable to determine absolute values of volume change prior to the permeability onset, and the presented information is limited to the time domain. The coincidence of traces obtained with WT and G113A MscS (Figure 1) suggests that inactivation does not contribute to the optical response reflecting efflux kinetics at this time scale.

In the absence of channels (KO cells) the light scattering response is longer and of larger amplitude (Figures 1 and 2). Two different phases are apparent: an initial shorter phase and a second longer one. As stated above, the first phase (0−50 ms) is similar in both WT and KO and likely represents initial swelling. The second longer stage in the KO strain most likely corresponds to excessive swelling and loss of membrane integrity. The scattering eventually reaches a lower level possibly due to more cytoplasmic depletion through a different pathway, likely nonspecific membrane "cracks". The slower scattering change suggests the overall permeability of the cracks is lower than that of the channel population. It is also possible that the rate of crack formation is slower than the opening rate of MscS, and this needs to be further quantified. The cracks also do not reseal since the scattering keeps changing throughout the entire 1 s observation period (Figure 1). A dramatic cell viability drop assayed under similar shock conditions (Figure 2C) indicates massive damage, which correlates with the amplitude of the "hump" in the difference traces (Figure 2A). Under 900 → 200 and 900 → 100 mOsm downshifts, only 14% and 2% of KO cells survive, whereas WT MscS rescues 95% and ~30% of cells, respectively, through MscS activation lasting ~50−100 ms based on the scattering responses.

The patch-clamp data collected on WT MscS (Figure 3) shows the channel population readily opens to machine-generated (10−15 ms raise time) pressure steps, and saturation is reached at ~8 mN/m (Figure 3C), substantially below lytic tensions of 12−15 mN/m, at which the large-conductance MscL channel activates.[12,30] After reaching the tension threshold of ~5 mN/m (Figure 3A−C), MscS population activates with a characteristic time of 1−3 ms, and the active fraction steeply grows with tension. Although the machine-limited pressure onset speed was too slow to determine the first-order rates of MscS activation, the data illustrate that the channel activity follows the tension increase with a minimal delay. The full response developing between 5 and 7 mN/m within 3 ms (Figure 3B,E) shows that MscS easily "keeps up" with the pressure buildup in the swelling bacterial cell and opens well before tension reaches lytic limit. The recently published fitting of MscS ramp responses with QuB suggested that the opening rate grows exponentially 12.7 times per 1 mN/m of tension increase.[34] This should provide the basis for estimation of the MscS opening latency at superthreshold tensions. The characteristic time of the MscS opening process itself has been estimated in high time resolution patch-clamp experiments to be shorter than 3 μs.[40]

When some cytoplasmic osmolytes are released and tension in the membrane drops, the channels close. We can confidently resolve the closing rate dependence on tension. When extrapolated to zero, it predicts that MscS can close within a millisecond. At 3 mN/m the population relaxes from the fully open to the closed state with a characteristic time of ~60 ms (Figure 3D,E). The scattering traces from WT-MscS (Figure 2) level off within ~50 ms of channel activation, which suggests that if a residual tension in the bacterial membrane persists after the shock, then it should be below 3 mN/m. Thus, comparing observed characteristic times from light-scattering and patch-clamp data gives us a range for membrane tension development in intact cells during osmotic shock *in vivo*.

As illustrated in Figure 4, MscS inactivation is a slow process. The channel does not respond to even supersaturating tension in the inactivated state.[15] It has been previously hypothesized that inactivation prevents cellular "bleeding" under prolonged exposure to hypotonic medium when tension may be near the activation threshold. Previous studies produced noninactivating and fast-inactivating[16,25] mutants which helped us address the biological role of inactivation and its slow kinetics. Ramps and steps were used to characterize the rate of inactivation (Figure 4). WT MscS readily responds to an abrupt tension onset, but most of the channels inactivate under 30−60 s ramps. For the fast-inactivating D62N mutant, it takes only a 5 s ramp to inactivate nearly the entire population, whereas G113A shows little inactivation under a 60 s ramp.

Single-step shocks performed with these mutants (Figure 5A) have indicated the viability of D62N is generally compromised compared to WT and G113A but is essentially independent of the length of exposure to the hypotonic medium. G113A survived long (60 min) shocks less than short shocks (1 min), which confirms inactivation assists recovery during or after the shock. The two-step shock protocol revealed the fast-inactivating mutant's vulnerability when mildly preshocked for a short period of time (15−60 s), which apparently drives most of the channel population to the inactivated state prior to stronger second shock. Importantly, extending the preshock time to 15 min restores D62N's ability survive likely because the cells adapted to the medium shock and the channels recovered. The above experiments illustrate why WT MscS inactivation is present yet slow. Indeed, after an abrupt down-shock and initial osmolyte release (when there is no real danger of membrane rupture), while the cell remains in a moderately hypotonc medium, the noninactivated MscS might be flickering and disrupting vital

gradients. Inactivation is highly beneficial for recovery. On the other hand, if inactivation is too fast, it may dangerously turn off the channel population during a gradual osmotic shock (such as in gentle rain), denying protection when conditions worsen.

In conclusion, the comparison of *in vivo* responses with characteristic MscS activation and closure times illustrate that abrupt shock fully activates MscS before pressure reaches lytic levels, followed by prompt closure upon partial osmotic equilibration of the cell. Under prolonged shocks, gradual inactivation prevents continuous channel activity and assists recovery. On the basis of *in vivo* assays conducted in the absence of MscL, inactivation appears to be a vital part of MscS' functional cycle and not a patch-clamp artifact.

■ ASSOCIATED CONTENT

Supporting Information. Steric feasibility of the D62−R131 salt bridged conformation illustrated in Figure S1 along with the technical details of the modeling process and a brief discussion of functional implications for the stability of the resting state. This material is available free of charge via the Internet at http://pubs.acs.org.

■ AUTHOR INFORMATION

Corresponding Author

*E-mail: sukharev@umd.edu. Phone: 301-405-6923. Fax: 301-314-9358.

Funding Sources

The work was supported by the NIH R01GM075225 grant to S.S.

■ ACKNOWLEDGMENT

The authors thank Dr. Ian Booth for the MJF465 strain and Dr. George Lorimer and Sarah Wehri for assistance with stopped flow experiments. The authors also thank Mrs. Naili Liu for general laboratory assistance and Dr. Kenjiro Yoshimura for the D62N mutant and helpful discussions.

■ ABBREVIATIONS

MscS, mechanosensitive channel of small conductance; MscL, mechanosensitive channel of large conductance; LB, Luria−Bertani medium; HEPES, 4-(2-hydroxyethyl)-1-piperazineethanesulfonic acid; HSPC, high-speed pressure-clamp apparatus.

■ REFERENCES

(1) Epstein, W. (2003) The roles and regulation of potassium in bacteria. *Prog. Nucleic Acid Res. Mol. Biol. 75*, 293–320.

(2) Wood, J. M., Bremer, E., Csonka, L. N., Kraemer, R., Poolman, B., van der Heide, T., and Smith, L. T. (2001) Osmosensing and osmoregulatory compatible solute accumulation by bacteria. *Comp. Biochem. Physiol., Part A: Mol. Integr. Physiol. 130*, 437–460.

(3) Schumann, U., Edwards, M. D., Rasmussen, T., Bartlett, W., van, W. P., and Booth, I. R. (2010) YbdG in Escherichia coli is a threshold-setting mechanosensitive channel with MscM activity. *Proc. Natl. Acad. Sci. U.S.A. 107*, 12664–12669.

(4) Li, Y., Moe, P. C., Chandrasekaran, S., Booth, I. R., and Blount, P. (2002) Ionic regulation of MscK, a mechanosensitive channel from Escherichia coli. *EMBO J. 21*, 5323–5330.

(5) Berrier, C., Besnard, M., Ajouz, B., Coulombe, A., and Ghazi, A. (1996) Multiple mechanosensitive ion channels from Escherichia coli, activated at different thresholds of applied pressure. *J. Membr. Biol. 151*, 175–187.

(6) Kung, C., Martinac, B., and Sukharev, S. (2010) Mechanosensitive channels in microbes. *Annu. Rev. Microbiol. 64*, 313–329.

(7) Booth, I. R., Edwards, M. D., and Miller, S. (2003) Bacterial ion channels. *Biochemistry 42*, 10045–10053.

(8) Levina, N., Totemeyer, S., Stokes, N. R., Louis, P., Jones, M. A., and Booth, I. R. (1999) Protection of Escherichia coli cells against extreme turgor by activation of MscS and MscL mechanosensitive channels: identification of genes required for MscS activity. *EMBO J. 18*, 1730–1737.

(9) Sukharev, S. (2002) Purification of the small mechanosensitive channel of Escherichia coli (MscS): the subunit structure, conduction, and gating characteristics in liposomes. *Biophys. J. 83*, 290–298.

(10) Blount, P., Sukharev, S. I., Moe, P. C., Schroeder, M. J., Guy, H. R., and Kung, C. (1996) Membrane topology and multimeric structure of a mechanosensitive channel protein of Escherichia coli. *EMBO J. 15*, 4798–4805.

(11) Sukharev, S. I., Blount, P., Martinac, B., Blattner, F. R., and Kung, C. (1994) A large-conductance mechanosensitive channel in E. coli encoded by mscL alone. *Nature 368*, 265–268.

(12) Belyy, V., Kamaraju, K., Akitake, B., Anishkin, A., and Sukharev, S. (2010) Adaptive behavior of bacterial mechanosensitive channels is coupled to membrane mechanics. *J. Gen. Physiol. 135*, 641–652.

(13) Moe, P., and Blount, P. (2005) Assessment of Potential Stimuli for Mechano-Dependent Gating of MscL: Effects of Pressure, Tension, and Lipid Headgroups. *Biochemistry 44*, 12239–12244.

(14) Stokes, N. R., Murray, H. D., Subramaniam, C., Gourse, R. L., Louis, P., Bartlett, W., Miller, S., and Booth, I. R. (2003) A role for mechanosensitive channels in survival of stationary phase: regulation of channel expression by RpoS. *Proc. Natl. Acad. Sci. U.S.A. 100*, 15959–15964.

(15) Akitake, B., Anishkin, A., and Sukharev, S. (2005) The "dashpot" mechanism of stretch-dependent gating in MscS. *J. Gen. Physiol. 125*, 143–154.

(16) Akitake, B., Anishkin, A., Liu, N., and Sukharev, S. (2007) Straightening and sequential buckling of the pore-lining helices define the gating cycle of MscS. *Nat. Struct. Mol. Biol. 14*, 1141–1149.

(17) Steinbacher, S., Bass, R., Strop, P., and Rees, D. C. (2007) Structures of the prokaryotic mechanosensitive channels MscL and MscS. *Mechanosensitive Ion Channels, Part A 58*, 1–24.

(18) Wang, W., Black, S. S., Edwards, M. D., Miller, S., Morrison, E. L., Bartlett, W., Dong, C., Naismith, J. H., and Booth, I. R. (2008) The structure of an open form of an E. coli mechanosensitive channel at 3.45 A resolution. *Science 321*, 1179–1183.

(19) Vasquez, V., Sotomayor, M., Cordero-Morales, J., Schulten, K., and Perozo, E. (2008) A structural mechanism for MscS gating in lipid bilayers. *Science 321*, 1210–1214.

(20) Vasquez, V., Sotomayor, M., Cortes, D. M., Roux, B., Schulten, K., and Perozo, E. (2008) Three-dimensional architecture of membrane-embedded MscS in the closed conformation. *J. Mol. Biol. 378*, 55–70.

(21) Anishkin, A., Akitake, B., and Sukharev, S. (2008) Characterization of the resting MscS: modeling and analysis of the closed bacterial mechanosensitive channel of small conductance. *Biophys. J. 94*, 1252–1266.

(22) Anishkin, A., Kamaraju, K., and Sukharev, S. (2008) Mechanosensitive channel MscS in the open state: modeling of the transition, explicit simulations, and experimental measurements of conductance. *J. Gen. Physiol. 132*, 67–83.

(23) Belyy, V., Anishkin, A., Kamaraju, K., Liu, N., and Sukharev, S. (2010) The tension-transmitting 'clutch' in the mechanosensitive channel MscS. *Nat. Struct. Mol. Biol. 17*, 451–458.

(24) Edwards, M. D., Li, Y., Kim, S., Miller, S., Bartlett, W., Black, S., Dennison, S., Iscla, I., Blount, P., Bowie, J. U., and Booth, I. R. (2005) Pivotal role of the glycine-rich TM3 helix in gating the MscS mechanosensitive channel. *Nat. Struct. Mol. Biol. 12*, 113–119.

(25) Nomura, T., Sokabe, M., and Yoshimura, K. (2008) Interaction between the cytoplasmic and transmembrane domains of the mechanosensitive channel MscS. *Biophys. J. 94*, 1638–1645.

(26) Edwards, M. D., Bartlett, W., and Booth, I. R. (2008) Pore mutations of the Escherichia coli MscS channel affect desensitization but not ionic preference. *Biophys. J. 94*, 3003–3013.

(27) Sotomayor, M., and Schulten, K. (2004) Molecular dynamics study of gating in the mechanosensitive channel of small conductance MscS. *Biophys. J. 87*, 3050–3065.

(28) Machiyama, H., Tatsumi, H., and Sokabe, M. (2009) Structural Changes in the Cytoplasmic Domain of the Mechanosensitive Channel MscS During Opening. *Biophys. J. 97*, 1048–1057.

(29) Okada, K., Moe, P. C., and Blount, P. (2002) Functional design of bacterial mechanosensitive channels. Comparisons and contrasts illuminated by random mutagenesis. *J. Biol. Chem. 277*, 27682–27688.

(30) Sukharev, S. I., Sigurdson, W. J., Kung, C., and Sachs, F. (1999) Energetic and spatial parameters for gating of the bacterial large conductance mechanosensitive channel, MscL. *J. Gen. Physiol. 113*, 525–540.

(31) de, Gier., J. (1993) Osmotic behaviour and permeability properties of liposomes. *Chem. Phys. Lipids 64*, 187–196.

(32) Beavis, A. D., Brannan, R. D., and Garlid, K. D. (1985) Swelling and contraction of the mitochondrial matrix. I. A structural interpretation of the relationship between light scattering and matrix volume. *J. Biol. Chem. 260*, 13424–13433.

(33) Koch, A. L., and Woeste, S. (1992) Elasticity of the sacculus of Escherichia coli. *J. Bacteriol. 174*, 4811–4819.

(34) Kamaraju, K., Gottlieb, P. A., Sachs, F., and Sukharev, S. (2010) Effects of GsMTx4 on Bacterial Mechanosensitive Channels in Inside-Out Patches from Giant Spheroplasts. *Biophys. J. 99*, 2870–2878.

(35) Bass, R. B., Strop, P., Barclay, M., and Rees, D. C. (2002) Crystal structure of Escherichia coli MscS, a voltage-modulated and mechanosensitive channel. *Science 298*, 1582–1587.

(36) Kamaraju, K., Belyy, V., Rowe, I., Anishkin, A., and Sukharev, S. (2011) The pathway and spatial scale for MscS inactivation. *J. Gen. Physiol.*

(37) Eze, M. O., and McElhaney, R. N. (1978) Stopped-flow spectrophotometric assay of glycerol permeation in Escherichia coli: applicability and limitations. *J. Gen. Microbiol. 105*, 233–242.

(38) Hubert, J. F., Duchesne, L., Delamarche, C., Vaysse, A., Gueune, H., and Raguenes-Nicol, C. (2005) Pore selectivity analysis of an aquaglyceroporin by stopped-flow spectrophotometry on bacterial cell suspensions. *Biol. Cell 97*, 675–686.

(39) Latimer, P. (1982) Light scattering and absorption as methods of studying cell population parameters. *Annu. Rev. Biophys. Bioeng. 11*, 129–150.

(40) Shapovalov, G., and Lester, H. A. (2004) Gating transitions in bacterial ion channels measured at 3 micros resolution. *J. Gen. Physiol. 124*, 151–161.